

## Towards the photophysical studies of humin by-products

Layla Filiciotto<sup>a</sup>, Gustavo de Miguel<sup>b</sup>, Alina M. Balu<sup>a</sup>, Antonio A. Romero<sup>a</sup>, Jan C. van der Waal<sup>c</sup> and Rafael Luque<sup>a\*</sup>

Received 00th January 20xx,  
Accepted 00th January 20xx

DOI: 10.1039/x0xx00000x

www.rsc.org/

**Biomass conversion into chemicals, materials and fuels emerged in the past decade as the most promising alternative to the current petroleum-based industry. However, chemocatalytic conversion of biomass and bio-derived sugars often leads to numerous side-products, such as humins. The limited characterization of humins materials restricts their study for possible future applications. Thus, herein photophysical studies on humins and separated humins fractions were carried out using steady-state and time-resolved fluorescence techniques. This paper aims to add to the literature important information for scientists involved in photophysical studies.**

The ongoing decrease of fossil feedstocks has pushed research towards the implementation of new technologies. Biomass conversion, for instance, has emerged in the past decade as an economically valid, environmental-friendly, sustainable alternative to the petroleum-based industry, thanks to its abundance, potential fast renewability, and compatibility with the current refinery technologies. However, biomass/sugars conversion lead to numerous side-products, limiting overall product yields and thus gravely effecting process economy. In particular, side-production of humins with yields of up to 50 wt% cause a major concern for biorefineries implementation[1-4]. Reduction of humins formation, in fact, has been one of the focuses in biomass conversion[5-7]; however, these studies often resort to cost ineffective technologies, such as the use of ionic liquids, recently proposed by Eminov et al.[7]. The authors of this manuscript, on the contrary, believe in the potential valorization of humin by-products to high-end chemicals, such as platform molecules, additives, materials, etc. In order to fully understand the applicability of these dark and insoluble compounds in-depth characterization is required.

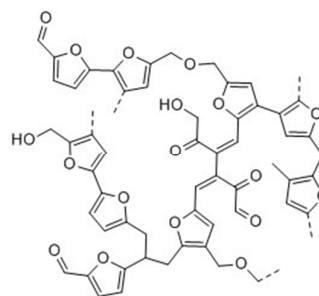


**Figure 1.** Humins structure adapted from ref. [16]

So far, humins formation mechanism and structure have not yet been unequivocally established, also due to the random character of these polymeric compounds. Numerous characterization and mechanistic studies have been performed on humins by means of IR, <sup>13</sup>C NMR, and pyrolysis-GC-MS [2, 8-20]. In general, a polymeric furanic-rich structure (270-650 g mol<sup>-1</sup>[16]) has been postulated, linked by short aliphatic chains, and acetal and/or ether functional group, leading to a highly oxygenated and possibly conjugated structure (Figure 1). The conjugated structure of humins suggests, therefore, possible fluorescence activity which could be applied to optical sciences. In fact, organic  $\pi$ -conjugated have gained increased attention thanks to their tunable optical and electronic properties, finding applications as organic photovoltaics, organic light-emitting devices, and organic field-effect transistors [21-25]. For this reason, fructose-derived humins (ca. 400 g mol<sup>-1</sup>[16]) solubilized in acetonitrile were investigated by means of steady-state and time-resolved fluorescence techniques. Moreover, these techniques have been applied to the separated organic and aqueous fractions of said solution, as the isolation of humins oligomers might yield to highly fluorescent molecules. In general, the aim of this manuscript is to give the reader new information on humin by-products, and possibly the inspiration towards the valorization of these compounds to high-end products.

<sup>a</sup> Departamento de Química Orgánica, Universidad de Córdoba, Campus de Rabanales, Edificio Marie Curie (C-3), Ctra Nnal IV-A, Km 396, Córdoba, Spain.

<sup>b</sup> Departamento de Química Física, Universidad de Córdoba, Campus de Rabanales, Edificio Marie Curie (C-3), Ctra Nnal IV-A, Km 396, Córdoba, Spain. E-mail: [g62alsor@uco.es](mailto:g62alsor@uco.es)

<sup>c</sup> Avantium Chemicals, Zekeringstraat 29, 1014 BV, Amsterdam, The Netherlands  
Electronic Supplementary Information (ESI) available: experimental section; absorption spectra of humins in solution, and of separated organic and aqueous fractions. See DOI: 10.1039/x0xx00000x

Figure S1 (*vide ESI*) displays the absorption spectrum (green line) of a dark solution of humins in a solvent with high polarity, acetonitrile (ACN). A featureless absorption signal with increasing values at the high-energy region is observed in the studied absorption range. Given the multicomponent character of the humins with likely presence of different polymeric furanic-rich species, the observed broad absorption signal can be explained as the overlapped contribution of different absorbing species. Figure 2A shows the emission spectra of the humins in ACN at different excitation wavelengths ( $\lambda_{\text{exc}}$ =250, 330 and 380 nm), revealing the presence of three emission peaks with maxima at 330, 405 and 500 nm. The emission peak at 500 nm is always detected regardless of the excitation wavelength, while the additional emission peaks at 330 and 405 nm appears exclusively upon excitation at 250 and 330 nm, respectively. Figure 2B also exhibits the excitation spectra at selected emission wavelengths ( $\lambda_{\text{em}}$ =325, 400 and 560 nm) indicating that three different absorption peaks are responsible for each emission signal. These results support our initial assumption that the absorption spectrum is composed of signals from different emitting species, i.e. fluorophores. Thus, the overall fluorescence behaviour can be easily accounted for the presence of three different fluorophores emitting at different wavelengths. The three species could be ascribed to different oligomeric fragments of the humins with varying length in the  $\pi$ -conjugated system including furanic rings and double bonds.

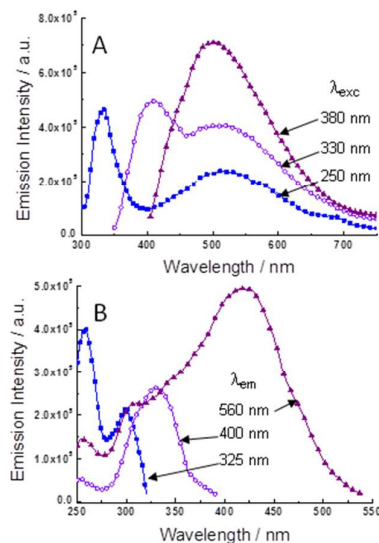


**Figure 2.** A) Emission spectra of humins in ACN at different excitation wavelengths.  $\lambda_{\text{exc}}$  = 250 (full blue squares), 330 (empty violet circles) and 380 nm (full purple triangles). B) Absorption and excitation spectra of the humins in ACN.  $\lambda_{\text{em}}$  = 330 (full blue squares), 400 (empty violet circles) and 560 nm (purple full triangles) in the excitation spectra.

With the aim of isolating each single fluorophore contained in the ACN solution, simple separations in biphasic systems have been performed in toluene/H<sub>2</sub>O and in pentane/H<sub>2</sub>O mixtures. When using toluene as the separating agent, all the aforementioned emission peaks were observed indicating that the three fluorophores are soluble in both solvents, despite

humins are reported to have poor solubility in H<sub>2</sub>O (1.4 mg/mL) [26].

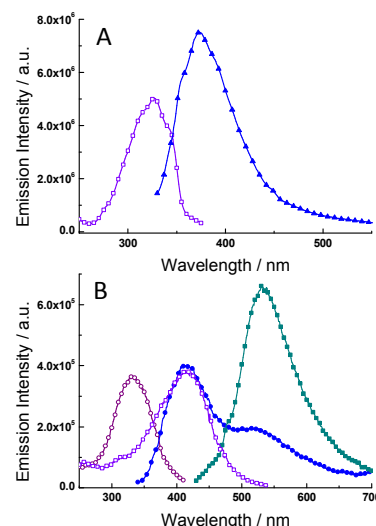


**Figure 3.** Excitation and emission spectra of the humins in the pentane phase (A) and in the aqueous phase (B). A)  $\lambda_{\text{em}}$  = 385 (empty violet squares) in the excitation spectrum and  $\lambda_{\text{exc}}$  = 310 (full blue triangles) in the emission spectrum. B)  $\lambda_{\text{em}}$  = 410 nm (empty purple circles) and  $\lambda_{\text{em}}$  = 560 nm (empty violet squares) in the excitation spectrum and  $\lambda_{\text{exc}}$  = 330 (full blue circles) and 410 nm (full green squares) in the emission spectrum.

The highly oxygenated (polar) and aromatic (non-polar) structure of humins denotes a certain amphiphilic character for these materials that certainly explains their solubility in the toluene/H<sub>2</sub>O mixed solution. Regarding the pentane/H<sub>2</sub>O solution, a partial separation of the components was observed in this case based on the absorption and emission spectra for each phase. Thus, Figure S1 shows the absorption spectra of the pentane and aqueous fractions with again a featureless signal in the H<sub>2</sub>O phase similar to that in ACN but with a more defined shape of the absorption signal in the organic phase. Thus, an apparent absorption band is visible at 365 nm with an additional signal around 325 nm in the pentane phase. Figure 3A exhibits the excitation ( $\lambda_{\text{em}}$  = 385 nm) and emission ( $\lambda_{\text{exc}}$  = 310 nm) spectra of the organic fraction. Excitation at different wavelengths was also performed giving no signal or the same emission spectrum as in  $\lambda_{\text{exc}}$  = 310 nm, which proves that only one fluorophore is found in the pentane phase (fluorophore 1). The emission band is centred at around 375 nm with a vibrational progression at shorter wavelength. The position of this emission peak does not match with those measured in the ACN solution, which might be explained due to the different dielectric constant in between both solvents (ACN vs. pentane) indicating a polarity-dependent deactivation process. Figure 3B displays the emission spectra for the aqueous phase at two excitation wavelengths,  $\lambda_{\text{exc}}$  = 330 and 410 nm. The excitation with the longer wavelength ( $\lambda_{\text{exc}}$  = 410 nm) generates an intense emission peak with maximum at 530 nm, while pumping with the shorter wavelength ( $\lambda_{\text{exc}}$  = 330 nm) produces an emission peak at 415 nm and a shoulder at around 525 nm that matches well with that peak obtained when exciting with

the longer wavelength ( $\lambda_{\text{exc}} = 410$  nm). This behaviour is accounted for the presence of two emitting species in the aqueous phase, fluorophore **2** and **3** with  $\lambda_{\text{em}} = 415$  and 530 nm, respectively. Moreover, the excitation spectra at  $\lambda_{\text{em}} = 410$  and 560 nm (Figure 3B) are almost identical to those observed in the ACN solution for the same  $\lambda_{\text{em}}$  which indicates that the same two fluorophores **2** and **3** are present in both solutions. The reported excitation and emission spectra of a highly-concentrated ACN solution of furfural exhibit similar peaks to those presented in this work, greatly supporting the presence of furfural-based derivatives in our humins samples [27]. Finally, based on the previous results we attribute the emission peak ( $\lambda_{\text{em}} = 375$  nm) in the pentane fraction to the same species responsible for the emission peak at  $\lambda_{\text{em}} = 330$  nm in the ACN solution (fluorophore **1**). These results prove the possibility of isolating the fluorophores with a simple mixture of water/pentane which could find application in organic electronics. Time-resolved fluorescence measurements were also performed to shed light into the photophysical deactivation of the different components in the humins solutions. Table 1 shows the derived fluorescence lifetimes ( $\tau$ ) obtained from both mono- or bi-exponential fits of the emission signals. In the ACN solution, the lifetime derived at  $\lambda_{\text{em}} = 420$  nm is 2.14 ns, which might be attributed to fluorophore **2** since it is essentially the only species emitting at this wavelength. The latter value is in good agreement with that obtained for the aqueous fraction at the same wavelength ( $\tau = 2.56$  ns) indicating that both signals arise from the same fluorophore **2**. The experimental emission signal at  $\lambda_{\text{em}} = 530$  nm of the ACN solution was fitted by using a bi-exponential function, with  $\tau_1 = 0.10$  ns and  $\tau_2 = 2.17$  ns. The origin of the double exponential behavior is unclear, but it might be tentatively assigned to the presence of a wide distribution of polymeric chains with different lengths that eventually produces a combination of emission lifetimes (fluorophore **3**). The same double exponential behavior was also detected in the aqueous fraction but with slightly lower lifetimes,  $\tau_1 = 0.10$  ns and  $\tau_2 = 1.20$  ns. Finally, the fit of the experimental emission signal of the pentane fraction gave a lifetime value of 1.70 ns, corresponding to the fluorophore **1** that is successfully separated in the organic phase.

**Table 1.** Lifetimes of the fluorophores derived from both mono- or bi-exponential fits of the experimental signals at  $\lambda_{\text{exc}} = 320$  or 440 nm and  $\lambda_{\text{em}} = 370$ , 420 or 530 nm.

	$\lambda_{\text{exc}}=320$ nm		$\lambda_{\text{exc}}=440$ nm	
	$\lambda_{\text{em}}=370$ nm		$\lambda_{\text{em}}=530$ nm	
	$\tau$ /ns	$\tau$ /ns	$\tau_1$ /ns	$\tau_2$ /ns
ACN solution		2.14	0.10 (0.30)	2.17 (0.70)
Pentane Fraction	1.70			
Aqueous Fraction		2.56	0.10 (0.15)	1.20 (0.85)

In summary, the results of the photophysical studies on humin by-products shows the presence of three distinctive fluorophores across the spectrum, of which one (fluorophore **1**, emitting in the UV region), can be isolated by a simple separation of the starting solution with a water/pentane

mixture. The time-resolved fluorescence studies showed both mono- and bi-exponential fits of the emission signals, with lifetimes of *ca.* 2 ns. In conclusion, a general elucidation of the photophysical properties of humin by-products in solution have been presented in the hopes of inspiring scientists in the investigation of these so-far waste materials for future optoelectronic applications.

## Notes and references

- L. Filiciotto, A.M. Balu, J.C. van der Waal, R. Luque, *Catal. Today*, 2017, DOI: 10.1016/j.cattod.2017.03.008.
- F.A.H. Rice, *J. Org. Chem.*, 1958, **23**, 465.
- T.M.C. Hoang, L. Lefferts and K. Seshan, *ChemSusChem*, 2013, **6**, 1651.
- I. V. Sumerskii, S.M. Krutov and M.Y. Zarubin, *Russ. J. Appl. Chem.*, 2010, **83**, 320.
- S. Wang, H. Lin, Y. Zhao, J. Chen and J. Zhou, *J. Anal. Appl. Pyrolysis*, 2016, **118**, 259.
- X. Tang, Y. Sun, X. Zeng, W. Hao, L. Lin and S. Liu, *Energy & Fuels*, 2014, **28**, 4251.
- S. Eminov, A. Brandt, J.D.E.T. Wilton-Ely and J.P. Hallett, *PLoS One*, 2016, **11**.
- I. V. Sumerskii, S.M. Krutov and M.Y. Zarubin, *Russ. J. Appl. Chem.*, 2010, **83**, 320.
- R.-J. van Putten, J.C. van der Waal, E. de Jong, C.B. Rasrendra, H.J. Heeres and J.G. de Vries, *Chem. Rev.*, 2013, **113**, 1499.
- F. Stankovikj, A.G. McDonald, G.L. Helms and M. Garcia-Perez, *Energy & Fuels*, 2016, **30**, 6505.
- J. Horvat, B. Klaić, B. Metelko and V. Šunjić, *Tetrahedron Lett.* 1985, **26**, 2111.
- S.K.R. Patil, J. Heltzel and C.R.F. Lund, *Energy & Fuels*, 2012, **26**, 5281.
- S.K.R. Patil and C.R.F. Lund, *Energy & Fuels*, 2011, **25**, 4745.
- J. Herzfeld, D. Rand, Y. Matsuki, E. Daviso, M. Mak-Jurkaskas and I. Mamajanov, *J. Phys. Chem. B.*, 2011, **115**, 5741.
- G.R. Akien, L. Qi and I.T. Horváth, *Chem. Commun.*, 2012, **48**, 5850.
- I. van Zandvoort, Y. Wang, C.B. Rasrendra, E.R.H. van Eck, P.C.A. Bruijninx, H.J. Heeres and B.M. Weckhuysen, *ChemSusChem*, 2013, **6**, 1745.
- I. van Zandvoort, E.R.H. van Eck, P. de Peinder, H.J. Heeres, P.C.A. Bruijninx and B.M. Weckhuysen, *ACS Sustain. Chem. Eng.*, 2015, **3**, 533.
- S. Wang, H. Lin, Y. Zhao, J. Chen and J. Zhou, *J. Anal. Appl. Pyrolysis.*, 2016, **118**, 259.
- G. Tsilomelekis, M.J. Orella, Z. Lin, Z. Cheng, W. Zheng, V. Nikolakis and D.G. Vlachos, *Green Chem.*, 2016, **18**, 1983.
- S. Wang, H. Lin, Y. Zhao, J. Chen and J. Zhou, *J. Anal. Appl. Pyrolysis*, 2016, **118**, 259–266.
- K.A. Mazzio and C.K. Luscombe, *Chem. Soc. Rev.*, 2015, **44**, 78.
- C. Zhong, C. Duan, F. Huang, H. Wu and Y. Cao, *Chem. Mater.* 2011, **23**, 326.
- J.-H. Jou, S. Kumar, A. Agrawal, T.-H. Li and S. Sahoo, *J. Mater. Chem. C*, 2015, **3**, 2974.
- C. Wang, H. Dong, W. Hu, Y. Liu and D. Zhu, *Chem. Rev.*, 2012, **112**, 2208.
- C. Zhang, P. Chen and W. Hu, *Chem. Soc. Rev.*, 2015, **44**, 2087.
- A. Mija, J.C. van der Waal, J.-M. Pin, N. Guigo and E. de Jong, *Constr. Buil. Mater.* 2016, **139**, 594..
- V. Gude, A. Das, T. Chatterjee and P. K. Mandal, *Phys. Chem. Chem. Phys.*, 2016, **18**, 28274.